# Computational and Biological Evaluation of $\beta$-adrenoreceptor Blockers as Promising Bacterial Anti-Virulence Agents

**Ahmad J. Almalki [1,*], Tarek S. Ibrahim [1], Sameh S. Elhady [2], Wael A. H. Hegazy [3] and Khaled M. Darwish [4,*]**

[1] Department of Pharmaceutical Chemistry, Faculty of Pharmacy, King Abdulaziz University, Jeddah, 21589, Saudi Arabia; tmabrahem@kau.edu.sa
[2] Department of Natural Products, Faculty of Pharmacy, King Abdulaziz University, Jeddah 21589, Saudi Arabia; ssahmed@kau.edu.sa
[3] Department of Microbiology and Immunology, Faculty of Pharmacy, Zagazig University, Zagazig, 44519, Egypt; waelmhegazy@daad-alumni.de
[4] Medicinal Chemistry Department, Faculty of Pharmacy, Suez Canal University, Ismailia 41522, Egypt
* Correspondence: ajalmalki@kau.edu.sa (A.J.A.); khaled_darwish@pharm.suez.edu.eg (K.M.D.)

## Additional Experimental Detail

1) **Table S1.** Descriptive ligand-TraR *A. tumefaciens* binding interactions through directed flexible docking protocol.
2) **Table S2.** Descriptive ligand-QscR *P. aeruginosa* binding interactions through directed flexible docking protocol.
3) **Table S3.** Descriptive ligand-CviR *C. violaceum* binding interactions through directed flexible docking protocol.
4) **Table S4.** Estimated ΔRMSF values for ligand-TraR *A. tumefaciens* proteins along the whole MD simulation.
5) **Table S5.** Estimated ΔRMSF values for ligand-QscR *P. aeruginosa* proteins along the whole MD simulation.
6) **Table S6.** Estimated ΔRMSF values for ligand-CviR *C. violaceum* proteins along the whole MD simulation.
7) **Table S7.** Sequences of the used primers in this study
8) **Figure S1.** 3D-representation of the binding site topology at the three bacterial LuxR-type quorum-sensing transcription factors.
9) **Figure S2.** Conformational analysis of simulated ligand-TraR *A. tumefaciens* protein complexes.
10) **Figure S3.** Conformational analysis of simulated ligand-QscR *P. aeruginosa* protein complexes.
11) **Figure S4.** Conformational analysis of simulated ligand-CviR *C. violaceum* protein complexes.
12) **Figure S5.** The architecture of three bacterial LuxR-type quorum sensing transcription factors.
13) **Figure S6.** Superimposing the co-crystallized (magenta sticks) and redocked (yellow sticks) ligands

**Table S1.** Descriptive ligand-TraR *A. tumefaciens* binding interactions through directed flexible docking protocol

| Compound | Ligand-target interaction description<br>[Type; Length (Å); Angle (°); Binding Residues] |
|---|---|
| **Propranolol** | Polar ; 2.8 **Å** ; Asp70 (sidechain C**O** $^-$ with **N**$^+$H$_2$)<br>H-bond ; 3.1 **Å** ; 121 ° ; Tyr53 (sidechain **O**H with N$^+$**H**H)<br>H-bond ; 1.9 **Å** ; 148 ° ; Thr129 (sidechain **O**H with propanol-O**H**)<br>π-π interaction ; 2.9 **Å** ; Tyr61<br>van der Waal ; 3.9 **Å** and 4.4 **Å;** Gln58 sidechain C*β* and C*δ* |
| **Pindolol** | Polar ; 2.7 **Å** ; Asp70 (sidechain C**O** $^-$ with **N**$^+$H$_2$)<br>H-bond ; 3.2 **Å** ; 159 ° ; Gln58 (mainchain C=**O** with indole N**H**)<br>H-bond ; 2.6 **Å** ; 127 ° ; Tyr61 (sidechain **O**H with propanol-O**H**)<br>π-π interaction ; 3.2 **Å** ; Tyr61 |
| **Timolol** | Polar ; 3.3 **Å** ; Asp70 (sidechain C**O** $^-$ with **N**$^+$H$_2$)<br>H-bond ; 2.0 **Å** ; 140 ° ; Tyr53 (sidechain O**H** with propanol-**O**H)<br>H-bond ; 3.1 **Å** ; 155 ° ; Trp57 (sidechain N**H** with aryloxy-**O**)<br>H-bond ; 2.9 **Å** ; 167 ° ; Thr129 (sidechain O**H** with ring **S**)<br>π-H interaction ; 4.1 **Å** ; Tyr61 |
| **Atenolol** | Polar ; 3.0 **Å** ; Asp70 (sidechain C**O** $^-$ with **N**$^+$H$_2$)<br>H-bond ; 1.8 **Å** ; 176 ° ; Tyr53 (sidechain O**H** with propanol-**O**H)<br>H-bond ; 2.9 **Å** ; 125 ° ; Gln58 (sidechain C=**O** with amide N**H**)<br>H-bond ; 3.1 **Å** ; 123 ° ; Tyr61 (sidechain O**H** with aryloxy-**O**)<br>H-bond ; 3.2 **Å** ; 135 ° ; Phe62 (mainchain N**H** with amide C=**O**)<br>H-bond ; 2.8 **Å** ; 121 ° ; Thr129 (sidechain O**H** with propanol-**O**H)<br>π-π interaction ; 3.1 **Å** ; Tyr61 |
| **Esmolol** | Polar ; 2.8 **Å** ; Asp70 (sidechain C**O** $^-$ with **N**$^+$H$_2$)<br>H-bond ; 2.3 **Å** ; 174 ° ; Tyr53 (sidechain O**H** with aryloxy-**O**)<br>H-bond ; 3.2 **Å** ; 131 ° ; Tyr53 (mainchain N**H** with ester C=**O**)<br>H-bond ; 3.1 **Å** ; 121 ° ; Thr51 (sidechain O**H** with ester C=**O**)<br>H-bond ; 3.0 **Å** ; 125 ° ; Phe62 (mainchain N**H** with ester **O**CH$_3$)<br>H-bond ; 2.8 **Å** ; 131 ° ; Thr129 (sidechain O**H** with aryloxy-**O**)<br>π-π interaction ; 4.0 **Å** ; Tyr61 |
| **Metoprolol** | Polar ; 2.8 **Å** ; Asp70 (sidechain C**O** $^-$ with **N**$^+$H$_2$)<br>H-bond ; 2.9 **Å** ; 170 ° ; Tyr53 (sidechain O**H** with aryloxy-**O**)<br>H-bond ; 3.0 **Å** ; 128 ° ; Thr51 (sidechain C=**O** with amide N**H**)<br>H-bond ; 2.9 **Å** ; 120 ° ; Trp85 (mainchain N**H** with propanol-**O**H)<br>H-bond ; 2.7 **Å** ; 147 ° ; Thr129 (sidechain O**H** with terminal methoxy **O**CH$_3$)<br>π-π interaction ; 3.2 **Å** ; Tyr61 |
| **HLC** | H-bond ; 3.2 **Å** ; 127 ° ; Asp70 (sidechain C=**O** with N**H**)<br>H-bond ; 2.1 **Å** ; 137 ° ; Tyr53 (sidechain O**H** with amide C=**O**)<br>H-bond ; 3.3 **Å** ; 153 ° ; Trp57 (sidechain N**H** with aryloxy-**O**)<br>H-bond ; 3.1 **Å** ; 120 ° ; Trp102 (sidechain O**H** with lactone C=**O**)<br>π-π interaction ; 4.1 **Å** ; Tyr61<br>van der Waal ; 3.5 **Å** and 4.8 **Å;** Gln58 sidechain C*β* and C*δ* |

**Table S2.** Descriptive ligand-QscR *P. aeruginosa* binding interactions through directed flexible docking protocol

| Compound | Ligand-target interaction description [Type; Length (Å); Angle (°); Binding Residues] |
|---|---|
| **Atenolol** | Polar ; 3.1 **Å** ; Asp75 (sidechain C**O**$^-$ with **N**$^+$H$_2$)<br>H-bond ; 2.6 **Å** ; 129 ° ; Ser38 (sidechain O**H** with aryloxy-**O**)<br>H-bond ; 3.3 **Å** ; 153 ° ; Tyr52 (sidechain **O**H with amide NH**H**)<br>H-bond ; 2.4 **Å** ; 154 ° ; Tyr58 (sidechain O**H** with propanol-**O**H)<br>H-bond ; 3.3 **Å** ; 137 ° ; Tyr66 (sidechain **O**H with propanol-O**H**)<br>π-H interaction ; 3.0 **Å** ; Trp90<br>π-H interaction ; 3.3 **Å** ; Trp102<br>van der Waals ; 3.6 **Å**; Arg42 sidechain C*β* |
| **Esmolol** | Polar ; 3.0 **Å** ; Asp75 (sidechain C**O**$^-$ with **N**$^+$H$_2$)<br>H-bond ; 2.1 **Å** ; 121 ° ; Ser38 (sidechain O**H** with propanol-**O**H)<br>H-bond ; 2.6 **Å** ; 132 ° ; Arg42 (mainchain N**H** with ester C=**O**)<br>H-bond ; 1.8 **Å** ; 147 ° ; Tyr58 (sidechain O**H** with propanol-**O**H)<br>H-bond ; 2.5 **Å** ; 129 ° ; Tyr66 (sidechain O**H** with aryloxy-**O**)<br>H-bond ; 2.7 **Å** ; 123 ° ; Ser129 (sidechain **O**H with propanol-O**H**)<br>π-π interaction ; 4.7 **Å** ; Phe54<br>π-H interaction ; 3.2 **Å** ; Trp90 |
| **Betaxolol** | Polar ; 3.3 **Å** ; Asp75 (sidechain C**O**$^-$ with **N**$^+$H$_2$)<br>H-bond ; 1.9 **Å** ; 137 ° ; Ser38 (sidechain O**H** with propanol-**O**H)<br>H-bond ; 1.7 **Å** ; 170 ° ; Tyr58 (sidechain O**H** with propanol-**O**H)<br>H-bond ; 2.2 **Å** ; 159 ° ; Tyr58 (sidechain **O**H with N$^+$**H**H)<br>H-bond ; 3.2 **Å** ; 129 ° ; Tyr66 (sidechain O**H** with aryloxy-**O**)<br>H-bond ; 3.2 **Å** ; 128 ° ; Met127 (mainchain N**H** with terminal-**O**-linker)<br>π-π interaction ; 4.5 **Å** ; Phe54<br>π-H interaction ; 3.4 **Å** ; Trp90 |
| **Bisoprolol** | Polar ; 3.3 **Å** ; Asp75 (sidechain C**O**$^-$ with **N**$^+$H$_2$)<br>H-bond ; 2.5 **Å** ; 123 ° ; Ser38 (sidechain O**H** with aryloxy-**O**)<br>H-bond ; 2.6 **Å** ; 148 ° ; Ser38 (sidechain **O**H with propanol-O**H**)<br>H-bond ; 1.9 **Å** ; 120 ° ; Tyr58 (sidechain O**H** with propanol-**O**H)<br>H-bond ; 2.1 **Å** ; 124 ° ; Asp75 (sidechain C=**O** with N$^+$**H**H)<br>H-bond ; 3.3 **Å** ; 121 ° ; Trp90 (sidechain N**H** with propanol-**O**H)<br>H-bond ; 3.0 **Å** ; 128 ° ; Ser129 (sidechain O**H** with aryloxy-**O**)<br>π-π interaction ; 4.4 **Å** ; Phe54<br>π-H interaction ; 3.6 **Å** ; Tyr66<br>π-H interaction ; 2.9 **Å** ; Trp90<br>van der Waal ; 3.7 **Å** and 4.2 **Å** ; Arg42 sidechain C*β* and C*δ* |
| **Metoprolol** | Polar ; 3.1 **Å** ; Asp75 (sidechain C**O**$^-$ with **N**$^+$H$_2$)<br>H-bond ; 3.0 **Å** ; 137 ° ; Ser38 (sidechain **O**H with propanol-O**H**)<br>H-bond ; 3.3 **Å** ; 129 ° ; Arg42 (mainchain N**H** with terminal-**O**-linker)<br>H-bond ; 3.3 **Å** ; 124 ° ; Tyr52 (sidechain N**H** with propanol-**O**H)<br>H-bond ; 2.6 **Å** ; 170 ° ; Tyr58 (sidechain **O**H with N$^+$**H**H)<br>H-bond ; 2.0 **Å** ; 128 ° ; Tyr58 (sidechain O**H** with propanol-**O**H)<br>H-bond ; 3.0 **Å** ; 127 ° ; Ser129 (sidechain **O**H with propanol-O**H**)<br>π-π interaction ; 4.9 **Å** ; Phe54<br>π-H interaction ; 3.1 **Å** ; Trp90<br>π-H interaction ; 3.5 **Å** ; Trp102<br>van der Waal ; 3.0 **Å** and 4.0 **Å** ; Arg42 sidechain C*β* and C*δ* |
| **Acebutolol** | Polar ; 3.2 **Å** ; Asp75 (sidechain C**O**$^-$ with **N**$^+$H$_2$)<br>H-bond ; 1.9 **Å** ; 128 ° ; Ser38 (sidechain O**H** with aryloxy-**O**) |

| | |
|---|---|
| | H-bond ; 2.1 **Å** ; 127 ° ; Ser38 (sidechain O**H** with propanol-**O**H)<br>H-bond ; 1.7 **Å** ; 154 ° ; Tyr58 (sidechain O**H** with propanol-**O**H)<br>H-bond ; 3.0 **Å** ; 137 ° ; Thr72 (mainchain N**H** with acetyl C=**O**)<br>H-bond ; 1.8 **Å** ; 157 ° ; Asp75 (sidechain C=**O** with $N^{+}$**H**H)<br>H-bond ; 3.3 **Å** ; 124 ° ; Met127 (mainchain N**H** with terminal amide C=**O**)<br>H-bond ; 3.0 **Å** ; 137 ° ; Ser129 (sidechain **O**H with propanol-O**H**)<br>π-π interaction ; 4.0 **Å** ; Phe54<br>π-H interaction ; 2.9 **Å** ; Tyr66<br>π-H interaction ; 2.9 **Å** ; Trp90<br>van der Waal ; 3.7 **Å** and 4.3 **Å** ; Arg42 sidechain Cβ and Cδ |
| **Labetalol** | H-bond ; 1.8 **Å** ; 149 ° ; Ser38 (sidechain O**H** with ethanol-**O**H)<br>H-bond ; 3.3 **Å** ; 137 ° ; Tyr58 (sidechain O**H** with ethanol-**O**H)<br>H-bond ; 2.3 **Å** ; 123 ° ; Trp62 (mainchain N**H** with carbamide C=**O**)<br>π-π interaction ; 3.3 **Å** ; Tyr52<br>π-H interaction ; 3.0 **Å** ; Phe54<br>π-H interaction ; 3.2 **Å** ; Tyr58<br>π-H interaction ; 2.5 **Å** ; Tyr66<br>van der Waal ; 3.3 **Å** ; Arg42 sidechain Cβ |
| **HLC** | H-bond ; 2.8 **Å** ; 128 ° ; Ser38 (sidechain O**H** with amide C=**O**)<br>H-bond ; 2.1 **Å** ; 148 ° ; Tyr58 (sidechain N**H** with aryloxy-**O**)<br>H-bond ; 2.0 **Å** ; 147 ° ; Trp62 (sidechain N**H** with lactone C=**O**)<br>H-bond ; 2.6 **Å** ; 149 ° ; Tyr66 (sidechain O**H** with amide C=**O**)<br>H-bond ; 2.4 **Å** ; 129 ° ; Asp75 (sidechain O**H** with amide C=**O**)<br>π-π interaction ; 4.5 **Å** ; Phe54<br>π-H interaction ; 2.7 **Å** ; Trp90<br>van der Waal ; 4.6 **Å** ; Arg42 sidechain Cβ |

**Table S3.** Descriptive ligand-CviR *C. violaceum* binding interactions through directed flexible docking protocol

| Compound | Ligand-target interaction description<br>[Type; Length (Å); Angle (°); Binding Residues] |
|---|---|
| **Pindolol** | Polar ; 3.0 **Å** ; Asp97 (sidechain C**O**$^-$ with **N**$^+$H$_2$)<br>H-bond ; 3.1 **Å** ; 141 ° ; Tyr80 (sidechain O**H** with aryloxy-**O**)<br>H-bond ; 3.3 **Å** ; 162 ° ; Tyr80 (sidechain O**H** with propanol-**O**H)<br>H-bond ; 3.2 **Å** ; 164 ° ; Asp97 (sidechain C=**O** with N$^+$**H**H)<br>H-bond ; 2.5 **Å** ; 125 ° ; Ser155 (sidechain **O**H with propanol-O**H**)<br>π-π interaction ; 4.2 **Å** ; Tyr80<br>π-π interaction ; 3.7 **Å** ; Tyr88<br>π-H interaction ; 3.4 **Å** ; Trp111 |
| **Atenolol** | Polar ; 3.2 **Å** ; Asp97 (sidechain C**O**$^-$ with **N**$^+$H$_2$)<br>H-bond ; 2.5 **Å** ; 163 ° ; Tyr80 (sidechain O**H** with propanol-**O**H)<br>H-bond ; 3.1 **Å** ; 144 ° ; Met89 (sidechain **S**CH$_3$ with terminal amide NH**H**)<br>H-bond ; 3.3 **Å** ; 128 ° ; Asp97 (sidechain C=**O** with N$^+$**H**H)<br>H-bond ; 2.5 **Å** ; 126 ° ; Ser155 (sidechain **O**H with propanol-O**H**)<br>H-bond ; 3.3 **Å** ; 125 ° ; Met253 (sidechain **S**CH$_3$ with terminal amide N**H**H)<br>π-π interaction ; 3.6 **Å** ; Tyr88<br>π-H interaction ; 2.9 **Å** ; Trp111 |
| **Esmolol** | Polar ; 2.7 **Å** ; Asp97 (sidechain C**O**$^-$ with **N**$^+$H$_2$)<br>H-bond ; 3.1 **Å** ; 171 ° ; Tyr80 (sidechain O**H** with propanol-**O**H)<br>H-bond ; 2.9 **Å** ; 174 ° ; Asp97 (sidechain C=**O** with N$^+$**H**H)<br>H-bond ; 2.7 **Å** ; 129 ° ; Ser155 (sidechain **O**H with propanol-O**H**)<br>π-π interaction ; 3.7 **Å** ; Tyr88<br>π-H interaction ; 3.2 **Å** ; Trp111 |
| **Betaxolol** | Polar ; 3.1 **Å** ; Asp97 (sidechain C**O**$^-$ with **N**$^+$H$_2$)<br>H-bond ; 3.3 **Å** ; 161 ° ; Tyr80 (sidechain O**H** with propanol-**O**H)<br>H-bond ; 3.2 **Å** ; 150 ° ; Asp97 (sidechain C=**O** with N$^+$**H**H)<br>H-bond ; 1.9 **Å** ; 149 ° ; Asp97 (sidechain C**O**$^-$ with propanol-O**H**)<br>π-π interaction ; 3.9 **Å** ; Tyr88<br>π-H interaction ; 3.0 **Å** ; Trp111 |
| **Bisoprolol** | Polar ; 2.7 **Å** ; Asp97 (sidechain C**O**$^-$ with **N**$^+$H$_2$)<br>H-bond ; 3.2 **Å** ; 172 ° ; Tyr80 (sidechain O**H** with propanol-**O**H)<br>H-bond ; 3.1 **Å** ; 164 ° ; Asp97 (sidechain C=**O** with N$^+$**H**H)<br>H-bond ; 3.1 **Å** ; 126 ° ; Ser155 (sidechain **O**H with propanol-O**H**)<br>π-π interaction ; 4.3 **Å** ; Tyr88<br>π-H interaction ; 3.3 **Å** ; Trp111 |
| **Metoprolol** | Polar ; 2.8 **Å** ; Asp97 (sidechain C**O**$^-$ with **N**$^+$H$_2$)<br>H-bond ; 3.3 **Å** ; 162 ° ; Tyr80 (sidechain O**H** with propanol-**O**H)<br>H-bond ; 3.3 **Å** ; 158 ° ; Asp97 (sidechain C=**O** with N$^+$**H**H)<br>H-bond ; 2.2 **Å** ; 134 ° ; Ser155 (sidechain **O**H with propanol-O**H**)<br>π-π interaction ; 3.8 **Å** ; Tyr88<br>π-H interaction ; 3.0 **Å** ; Trp111 |
| **Acebutolol** | Polar ; 3.3 **Å** ; Asp97 (sidechain C**O**$^-$ with **N**$^+$H$_2$)<br>H-bond ; 3.2 **Å** ; 142 ° ; Tyr80 (sidechain O**H** with aryloxy-**O**)<br>H-bond ; 3.3 **Å** ; 165 ° ; Trp84 (sidechain N**H** with propanol-**O**H)<br>H-bond ; 2.9 **Å** ; 128 ° ; Tyr88 (sidechain O**H** with propanol-**O**H)<br>H-bond ; 1.6 **Å** ; 168 ° ; Asp97 (sidechain C=**O** with propanol-O**H**)<br>π-π interaction ; 4.5 **Å** ; Tyr80<br>π-π interaction ; 3.8 **Å** ; Tyr88<br>π-H interaction ; 3.2 **Å** ; Trp111 |
| **Labetalol** | Polar ; 2.2 **Å** ; Asp97 (sidechain C**O**$^-$ with **N**$^+$H$_2$)<br>H-bond ; 3.3 **Å** ; 162 ° ; Tyr80 (sidechain O**H** with ethanol-**O**H) |

| | |
|---|---|
| | H-bond ; 2.4 **Å** ; 162 ° ; Trp84 (sidechain N**H** with phenyl-4-**O**H)<br>H-bond ; 2.1 **Å** ; 158 ° ; Asp97 (sidechain C=**O** with $N^{+}$**H**H)<br>H-bond ; 3.2 **Å** ; 134 ° ; Met135 (sidechain **S**$CH_3$ with phenyl-4-O**H**)<br>π-H interaction ; 3.8 **Å** ; Tyr88<br>π-π interaction ; 3.0 **Å** ; Trp111 |
| **HLC** | H-bond ; 2.5 **Å** ; 158 ° ; Tyr80 (sidechain O**H** with amide C=**O**)<br>H-bond ; 2.0 **Å** ; 169 ° ; Trp84 (sidechain N**H** with lactone C=**O**)<br>H-bond ; 2.8 **Å** ; 121 ° ; Trp84 (sidechain N**H** with lactone **O**)<br>H-bond ; 2.3 **Å** ; 161 ° ; Asp97 (sidechain C=**O** with amide N**H**)<br>π-H interaction ; 4.0 **Å** ; Tyr80<br>π-π interaction ; 5.1 **Å** ; Tyr88<br>π-H interaction ; 2.8 **Å** ; Trp111 |

**Table S4.** Estimated ΔRMSF[a] values for ligand-TraR *A. tumefaciens* proteins along the whole MD simulation.

| Pocket Residues | HLC | Comp.1 | Comp.2 | Comp.8 | Comp.10 | Comp.11 | Comp.14 |
|---|---|---|---|---|---|---|---|
| **Ala38** | -0.08 | -0.29 | -0.15 | 0.08 | 0.26 | 0.10 | 0.22 |
| **Tyr39** | 0.06 | -0.1 | 0.03 | 0.21 | **0.35** | 0.16 | 0.27 |
| **Leu40** | 0.18 | -0.03 | 0.10 | 0.1 | **0.36** | 0.05 | 0.20 |
| **Thr51** | **0.53** | 0.23 | **0.39** | **0.71** | **0.92** | **0.67** | **0.73** |
| **Tyr53** | **0.31** | -0.18 | 0.01 | **0.38** | **0.62** | 0.24 | **0.72** |
| **Trp57** | -0.23 | -0.63 | -0.64 | -0.17 | 0.11 | -0.39 | -0.01 |
| **Tyr61** | -0.59 | -0.98 | -1.07 | -0.70 | -0.56 | -0.91 | -0.61 |
| **Phe62** | -1.04 | -1.47 | -1.61 | -1.18 | -0.97 | -1.39 | -1.15 |
| **Asp70** | 0.19 | **0.32** | 0.25 | **0.37** | **0.50** | 0.27 | **0.51** |
| **Val72** | **0.61** | **0.60** | **0.45** | -0.26 | **0.62** | **0.29** | **0.46** |
| **Trp85** | -0.26 | -0.29 | -0.14 | -0.93 | 0.16 | -0.22 | -0.01 |
| **Phe101** | **0.35** | **0.64** | **0.36** | **0.31** | **0.51** | **0.46** | **0.55** |
| **Tyr102** | **0.49** | **0.73** | **0.63** | **0.31** | **0.73** | **0.35** | **0.67** |
| **Ala105** | **1.27** | **1.39** | **1.40** | **1.25** | **1.60** | **1.36** | **1.56** |
| **Ile110** | **1.08** | **1.12** | **1.29** | **1.06** | **1.55** | **1.31** | **1.47** |
| **Thr115** | **1.48** | **1.53** | **1.55** | **1.36** | **1.69** | **1.55** | **1.58** |
| **Met127** | -0.09 | -0.05 | -0.06 | -0.05 | 0.07 | -0.10 | -0.06 |
| **Phe128** | -0.25 | -0.25 | -0.17 | -0.06 | 0.08 | -0.09 | -0.05 |
| **Thr129** | -0.38 | -0.36 | -0.28 | -0.31 | 0.00 | -0.16 | -0.11 |

[a] Relative difference root-mean-square fluctuation (ΔRMSF) was estimated for each ligand-associated TraR protein relative to the apo/unliganded state. Residues showing significant immobility are with ΔRMSF > 0.30 Å cut-off are in bold red color and highlighted.

**Table S5.** Estimated ΔRMSF[a] values for ligand-QscR *P. aeruginosa* proteins along the whole MD simulation.

| Pocket Residues | HLC | Comp.10 | Comp.11 | Comp.12 | Comp.13 | Comp.14 | Comp.17 | Comp.21 |
|---|---|---|---|---|---|---|---|---|
| **Ser38** | 0.18 | 0.08 | **0.37** | **0.37** | 0.21 | 0.12 | **0.35** | 0.27 |
| **Phe39** | 0.00 | -0.10 | **0.32** | **0.31** | 0.15 | 0.08 | 0.18 | 0.19 |
| **Gly40** | -0.05 | -0.46 | 0.11 | 0.14 | -0.13 | -0.03 | 0.07 | -0.11 |
| **Ala41** | 0.14 | -0.04 | 0.27 | **0.31** | 0.17 | 0.14 | 0.26 | 0.17 |
| **Arg42** | 0.02 | 0.13 | **0.34** | **0.34** | **0.32** | **0.30** | **0.33** | 0.06 |
| **Tyr52** | -0.64 | -0.61 | -0.33 | -0.34 | -0.25 | -0.14 | -0.24 | -0.98 |
| **His53** | -0.25 | -0.44 | -0.16 | -0.18 | -0.26 | -0.22 | -0.15 | -0.59 |
| **Phe54** | -0.44 | -0.41 | -0.20 | -0.11 | -0.36 | -0.28 | -0.21 | -0.32 |
| **Ser56** | -0.51 | -0.25 | 0.02 | -0.04 | -0.14 | -0.25 | -0.08 | -0.10 |
| **Tyr58** | -0.10 | -0.21 | 0.11 | -0.12 | -0.09 | -0.31 | 0.13 | -0.10 |
| **Trp62** | -0.08 | 0.03 | 0.28 | **0.32** | 0.01 | 0.02 | **0.44** | 0.19 |
| **Lys63** | -0.40 | -0.42 | -0.03 | -0.13 | -0.71 | -0.22 | 0.08 | -0.12 |
| **Tyr66** | -0.77 | -0.49 | -0.20 | -0.18 | -0.81 | -0.04 | 0.00 | -0.30 |
| **Ile67** | -1.19 | -0.89 | -0.43 | -0.53 | -1.49 | -0.33 | -0.19 | -0.69 |
| **Thr72** | -0.88 | -1.01 | -0.57 | -0.64 | -1.30 | -0.37 | -0.41 | -0.54 |
| **Asp75** | **0.31** | **0.43** | **0.31** | **0.37** | **0.47** | 0.28 | 0.25 | 0.07 |
| **Ile77** | **0.31** | 0.13 | **0.45** | **0.43** | 0.13 | **0.32** | **0.40** | **0.41** |
| **Val78** | **0.37** | 0.18 | **0.59** | **0.54** | 0.24 | **0.46** | **0.51** | **0.47** |
| **Leu82** | **0.36** | **0.33** | **0.53** | **0.47** | 0.19 | **0.40** | **0.53** | 0.07 |
| **Trp90** | **0.34** | **0.37** | **0.43** | **0.47** | **0.35** | 0.22 | **0.45** | **0.49** |
| **Phe101** | -0.49 | -0.20 | -0.07 | 0.06 | -0.12 | -0.13 | 0.10 | 0.12 |
| **Trp102** | -0.11 | 0.11 | 0.24 | **0.35** | 0.22 | 0.14 | **0.38** | **0.48** |
| **Ala105** | -0.58 | -0.45 | -0.23 | -0.17 | -0.30 | -0.62 | -0.16 | -0.19 |
| **Ile110** | -0.05 | 0.06 | 0.25 | 0.26 | 0.12 | -0.23 | **0.32** | 0.25 |
| **Ile125** | **0.74** | **0.63** | **0.86** | **0.88** | **0.67** | **0.71** | **0.88** | **0.74** |
| **Met127** | **0.82** | **0.55** | **0.93** | **0.98** | **0.79** | **0.73** | **0.93** | **0.86** |
| **Ser129** | **0.91** | **0.72** | **1.02** | **1.01** | **0.84** | **0.77** | **1.01** | **0.92** |

[a] Relative difference root-mean-square fluctuation (ΔRMSF) was estimated for each ligand-associated QscR protein relative to the apo/unliganded state. Residues showing significant immobility are with ΔRMSF > 0.30 Å cut-off are in bold red color and highlighted.

**Table S6.** Estimated ΔRMSF[a] values for ligand-CviR *C. violaceum* proteins along the whole MD simulation.

| Pocket Residues | HLC | Comp.2 | Comp.10 | Comp.11 | Comp.12 | Comp.13 | Comp.14 | Comp.17 | Comp.21 |
|---|---|---|---|---|---|---|---|---|---|
| **Leu57** | **0.80** | **0.96** | **0.43** | **0.59** | **0.56** | **0.70** | **0.49** | **0.70** | **0.32** |
| **Ile69** | -0.72 | -0.62 | -0.29 | -0.49 | -0.60 | -0.71 | -0.51 | -0.41 | -0.85 |
| **Gln70** | -0.87 | -0.75 | -0.49 | -0.78 | -0.62 | -0.90 | -0.78 | -0.62 | -1.25 |
| **Arg71** | -0.70 | -0.66 | -0.43 | -0.54 | -0.48 | -0.78 | -0.64 | -0.51 | -1.16 |
| **Leu72** | 0.18 | 0.28 | 0.25 | 0.22 | 0.13 | 0.26 | 0.28 | 0.18 | 0.13 |
| **Val75** | -0.14 | -0.08 | 0.23 | 0.18 | -0.40 | 0.02 | 0.21 | **0.36** | 0.12 |
| **Asn77** | -0.72 | -0.62 | -0.29 | -0.49 | -0.6 | -0.71 | -0.51 | -0.41 | -0.85 |
| **Tyr80** | **0.49** | **0.53** | **0.93** | **0.74** | **0.32** | **0.72** | **0.88** | **1.00** | **0.94** |
| **Trp84** | 0.26 | 0.08 | **0.61** | 0.28 | 0.15 | **0.30** | **0.53** | **0.47** | **0.46** |
| **Leu85** | **0.31** | 0.04 | **0.57** | 0.04 | 0.02 | 0.28 | **0.40** | **0.36** | **0.63** |
| **Tyr88** | 0.10 | **0.64** | 0.06 | **0.41** | **0.43** | 0.05 | 0.07 | 0.12 | **0.36** |
| **Met89** | **0.52** | 0.10 | **0.56** | 0.10 | 0.01 | **0.40** | **0.40** | **0.43** | **0.68** |
| **Ala94** | 0.23 | -0.51 | 0.04 | -0.06 | -0.31 | -0.23 | 0.26 | -0.17 | 0.21 |
| **Gln95** | 0.25 | -0.41 | 0.20 | -0.07 | -0.34 | -0.17 | 0.27 | 0.12 | 0.16 |
| **Asp97** | **0.43** | **1.07** | **0.53** | **0.98** | **1.18** | **0.83** | **0.50** | **0.67** | 0.29 |
| **Pro98** | -0.37 | -0.84 | -0.39 | -0.82 | -0.99 | -0.74 | -0.50 | -0.47 | -0.53 |
| **Ile99** | **0.44** | **0.83** | **0.64** | **0.49** | **1.05** | 0.28 | **0.73** | 0.28 | **0.62** |
| **Leu100** | **0.29** | **0.32** | **0.70** | 0.29 | **1.07** | **0.30** | 0.28 | 0.27 | **1.00** |
| **Arg101** | -0.67 | -0.93 | -0.50 | -0.89 | -0.83 | -0.81 | -0.62 | -0.78 | -0.79 |
| **Trp111** | **1.25** | **0.96** | **0.66** | **0.36** | **0.60** | **0.68** | **0.75** | **0.87** | **0.61** |
| **Phe115** | 0.21 | **0.30** | **0.43** | **0.49** | **0.51** | **0.32** | **0.49** | **0.33** | **0.38** |
| **Phe126** | -0.70 | -1.33 | -0.41 | -1.07 | -1.25 | -0.72 | -0.97 | -0.97 | -0.80 |
| **Ala130** | -0.55 | -1.09 | -0.25 | -0.99 | -1.12 | -0.61 | -0.77 | -0.46 | -0.52 |
| **Met135** | -0.16 | -0.59 | 0.14 | -0.59 | -0.57 | -0.27 | -0.36 | 0.16 | 0.02 |
| **Thr140** | -0.81 | -1.16 | -0.52 | -1.08 | -1.07 | -0.84 | -1.11 | -0.77 | -0.71 |
| **Ile153** | **1.38** | **1.59** | **0.78** | **1.16** | **1.08** | **1.23** | **1.24** | **1.17** | **1.31** |
| **Ser155** | **0.84** | **0.71** | **0.38** | -0.04 | **0.65** | **0.66** | -0.21 | -0.03 | -0.21 |
| **Val250** | **1.31** | 0.22 | 0.08 | **2.37** | **0.52** | **0.64** | **1.41** | **0.85** | **0.38** |

[a] Relative difference root-mean-square fluctuation (ΔRMSF) was estimated for each ligand-associated CviR protein relative to the apo/unliganded state. Residues showing significant immobility are with ΔRMSF > 0.30 Å cut-off are in bold red color and highlighted.

**Table S7.** Sequences of the used primers in this study

| Target gene | Sequence (5′–3′) | Reference |
|---|---|---|
| ***lasI*** | **For:** CTACAGCCTGCAGAACGACA<br>**Rev:** ATCTGGGTCTTGGCATTGAG | [1] |
| ***lasR*** | **For:** ACGCTCAAGTGGAAAATTGG<br>**Rev:** GTAGATGGACGGTTCCCAGA | [1] |
| ***rhlI*** | **For:** CTCTCTGAATCGCTGGAAGG<br>**Rev:** GACGTCCTTGAGCAGGTAGG | [2] |
| ***rhlR*** | **For:** AGGAATGACGGAGGCTTTTT<br>**Rev:** CCCGTAGTTCTGCATCTGGT | [1] |
| ***pqsA*** | **For:** TTCTGTTCCGCCTCGATTTC<br>**Rev:** AGTCGTTCAACGCCAGCAC | [1] |
| ***pqsR*** | **For:** AACCTGGAAATCGACCTGTG<br>**Rev:** TGAAATCGTCGAGCAGTACG | [1] |
| ***rpoD*** | **For:** GGGCGAAGAAGGAAATGGTC<br>**Rev:** CAGGTGGCGTAGGTGGAGAAC | [1] |
| ***qseC*** | **For:** GGTACCAAATTGACGCAACGTCTCAG<br>**Rev:** GAATTCGCCCAACTTACTACGGCCTC | [3] |
| ***qseE*** | **For:** GGTACCAGCGACACGTTGAAGCGC<br>**Rev:** GAATTCGCGTGTTTGTCAGATGCAGG | [3] |
| ***gyrB*** | **For:** GTGATCAGCGTCGCCACT<br>**Rev:** GCGCGGTGATCAGCGTC | [4] |

**References**


1. Hegazy, W. A. H.; Khayat, M. T.; Ibrahim, T. S.; Nassar, M. S.; Bakhrebah, M. A.; Abdulaal, W. H.; Alhakamy, N. A.; Bendary, M. M., Repurposing Anti-diabetic Drugs to Cripple Quorum Sensing in Pseudomonas aeruginosa. *Microorganisms* **2020,** 8, (9).
2. Aldawsari, M. F.; Khafagy, E. S.; Saqr, A. A.; Alalaiwe, A.; Abbas, H. A.; Shaldam, M. A.; Hegazy, W. A. H.; Goda, R. M., Tackling Virulence of Pseudomonas aeruginosa by the Natural Furanone Sotolon. *Antibiotics (Basel)* **2021,** 10, (7).
3. Moreira, C. G.; Sperandio, V., Interplay between the QseC and QseE bacterial adrenergic sensor kinases in Salmonella enterica serovar Typhimurium pathogenesis. *Infect Immun* **2012,** 80, (12), 4344-53.
4. Askoura, M.; Hegazy, W. A. H., Ciprofloxacin interferes with Salmonella Typhimurium intracellular survival and host virulence through repression of Salmonella pathogenicity island-2 (SPI-2) genes expression. *Pathog Dis* **2020,** 78, (1).

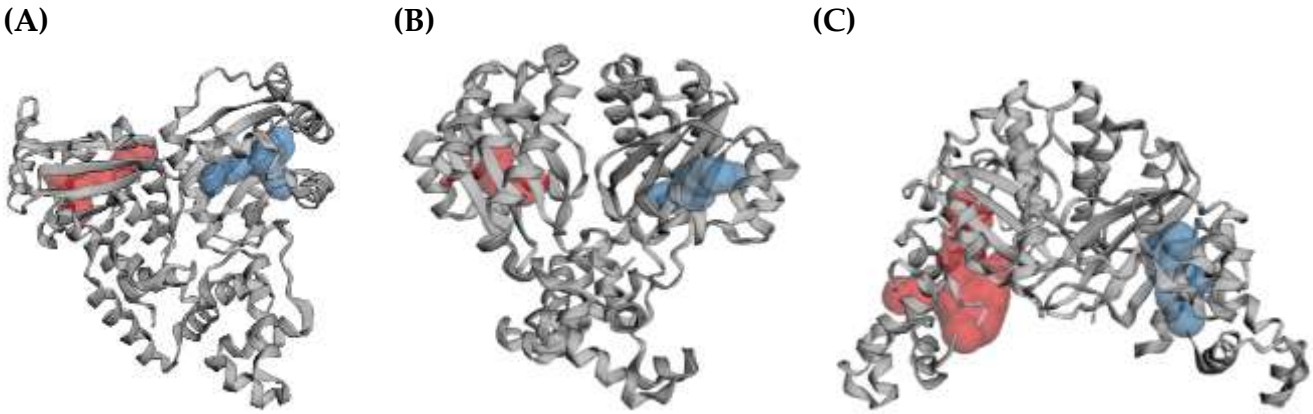


**Figure S1.** 3D-representation of the binding site topology at the three bacterial LuxR-type quorum-sensing transcription factors. (**A**) TraR *Agrobacterium tumefaciens*; (**B**) QscR *Pseudomonas aeruginosa*; (**C**) CviR *Chromobacterium violaceum*. Putative pockets were calculated via the on-line Computed Atlas of Surface Topography of proteins (CASTp; http://sts.bioe.uic.edu/castp/index.html) using 1.4 Å radius probe, visualized as surface 3D-representation, and colored in different colors (blue and red) for each target protomer. Estimated pocket area and volume were analytically calculated using the Richard's solvent-accessible surface model.

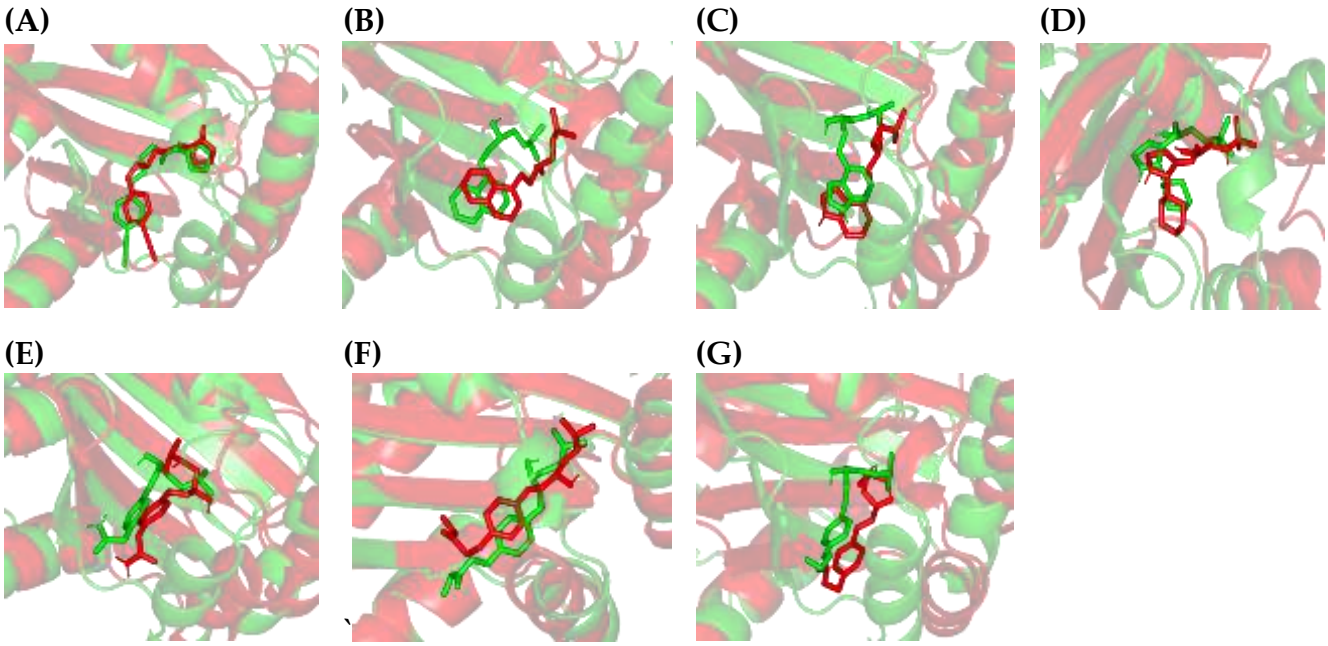


**Figure S2.** Conformational analysis of simulated ligand-TraR *A. tumefaciens* protein complexes. (**A**) HLC; (**B**) Comp.**1**; (**C**) Comp.**2**; (**D**) Comp.**8**; (**E**) Comp.**10**; (**F**) Comp.**11**; (**G**) Comp.**14**. Overlaid snapshots of the ligand-protein complex at 0 ns and 100 ns of the MD simulation runs. The TraR *A. tumefaciens* proteins are represented in green and red cartoon 3D-representation corresponding to initial and last extracted frames, respectively. Ligands (sticks) are presented in colors corresponding to their respective extracted frames.

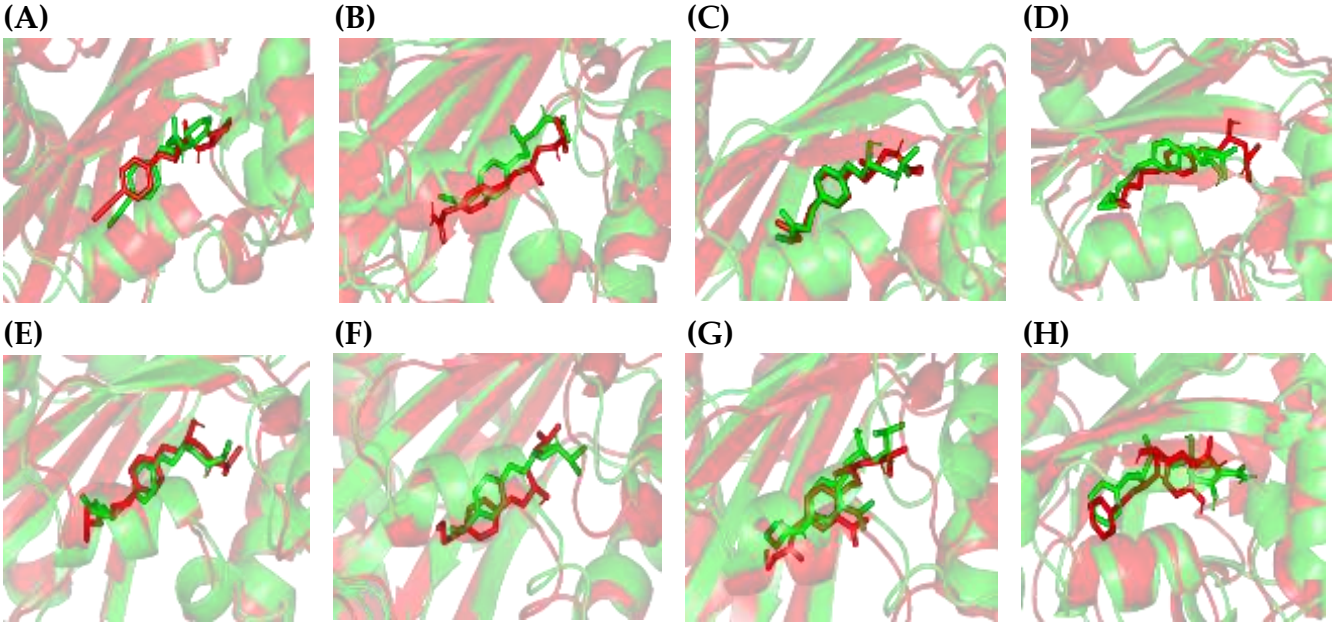


**Figure S3.** Conformational analysis of simulated ligand-QscR *P. aeruginosa* protein complexes. (**A**) HLC; (**B**) Comp.**10**; (**C**) Comp.**11** (**D**) Comp.**12**; (**E**) Comp.**13**; (**F**) Comp.**14**; (**G**) Comp.**17**; (**H**) Comp.**21**. Overlaid snapshots of the ligand-protein complex at 0 ns and 100 ns of the MD simulation runs. The QscR *P. aeruginosa* proteins are represented in green and red cartoon 3D-representation corresponding to initial and last extracted frames, respectively. Ligands (sticks) are presented in colors corresponding to their respective extracted frames.

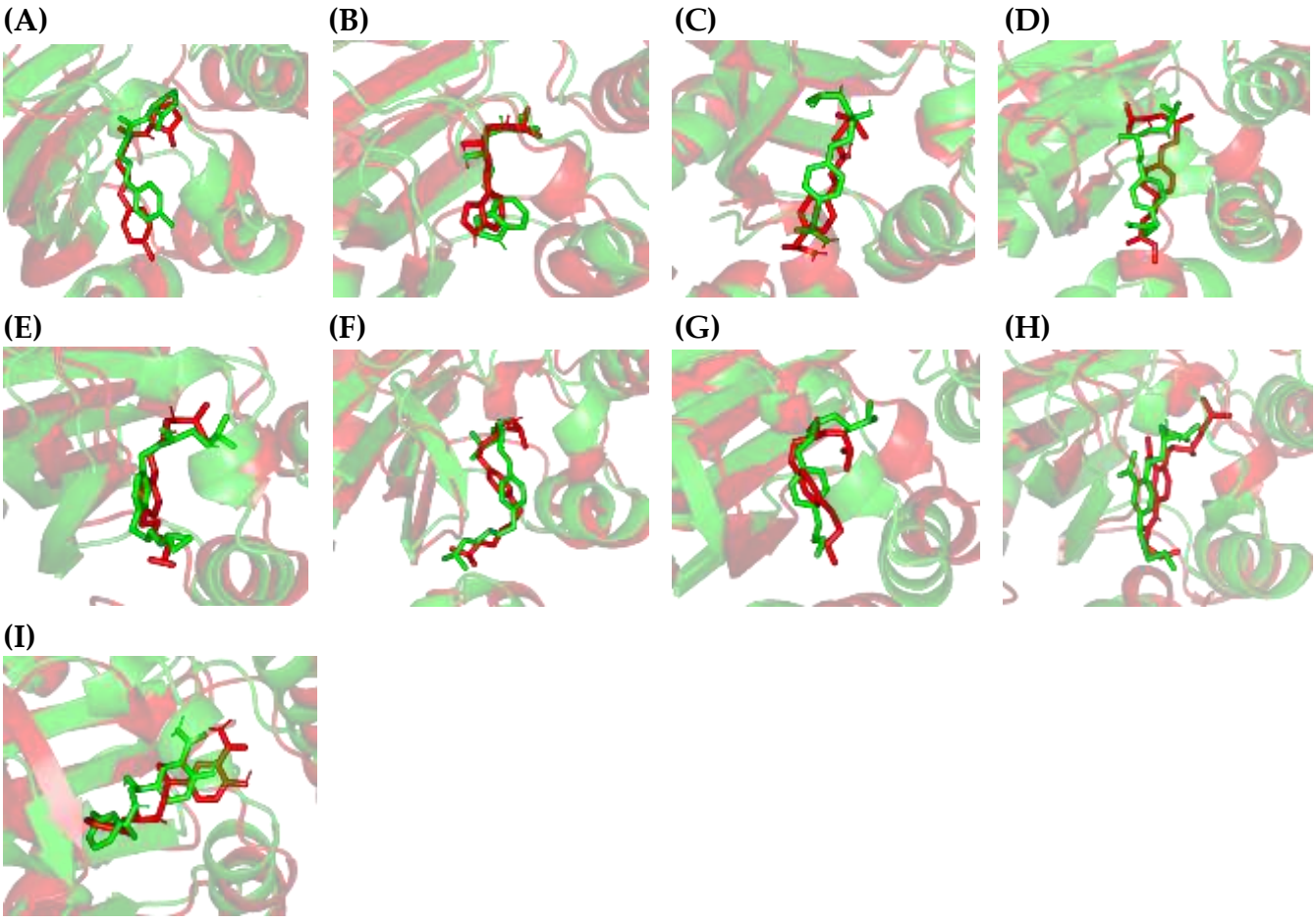


**Figure S4.** Conformational analysis of simulated ligand-CviR *C. violaceum* protein complexes. (**A**) HLC; (**B**) Comp.**2**; (**C**) Comp.**10** (**D**) Comp.**11**; (**E**) Comp.**12**; (**F**) Comp.**13**; (**G**) Comp.**14**; (**H**) Comp.**17**; (**I**) Comp.**21**. Overlaid snapshots of the ligand-protein complex at 0 ns and 100 ns of the MD simulation runs. The CviR *C. violaceum* proteins are represented in green and red cartoon 3D-representation corresponding to initial and last extracted frames, respectively. Ligands (sticks) are presented in colors corresponding to their respective extracted frames.

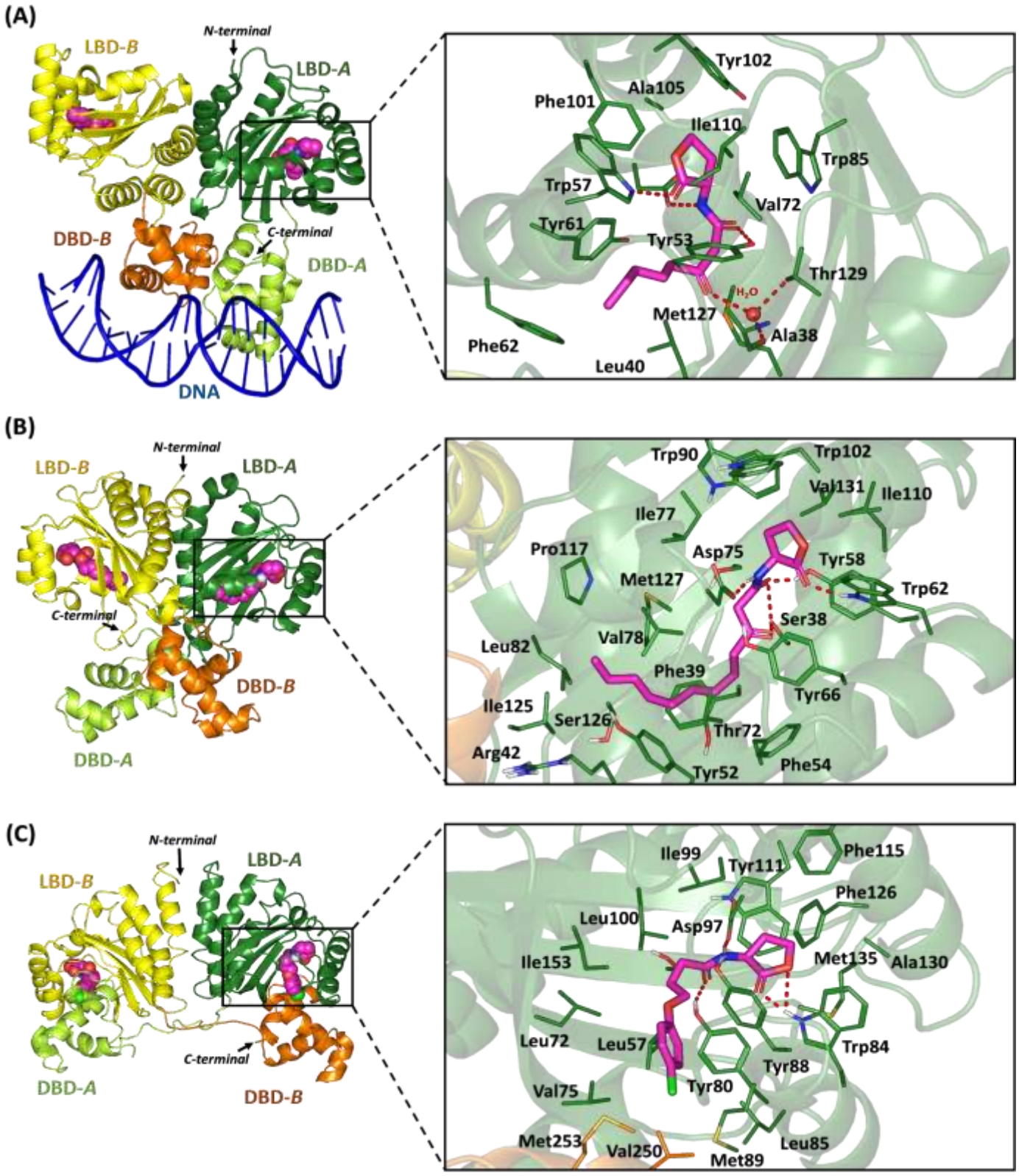


**Figure S5.** The architecture of three bacterial LuxR-type quorum sensing transcription factors. Left panels are overall cartoon representation of the TraR from *A. tumefaciens* PDB entry: 1L3L (**A**), QscR from *P. aeruginosa* PDB entry: 3SZT (**B**), and CviR from *C. violaceum* PDB entry: 3QP5 (**C**), where each protomer is colored differently in regard to its ligand-binding domain (LBD) and DNA-binding domain (DBD) as light/dark green and dark/light orange for protomer-A and -B, respectively. Ligands are represented as magenta spheres, whereas DNA is presented as blue cartoon only at *A. tumefaciens* TraR crystal structure. Right panels are the overlay of each co-crystallized ligand (magenta sticks) at the binding site of its respective bacterial LuxR-type quorum sensing transcription factor; (**A**) O-C8-HSL, (**B**) O-C12-HSL, and (**C**) HLC. Polar interactions, represented as hydrogen bonds, are illustrated as red dashed-lines and only residues (green lines), located within 4 Å radius of bound ligand, are displayed and labeled with sequence number. Crystallized water molecule bridging the ligand/residue interactions is shown as red sphere.

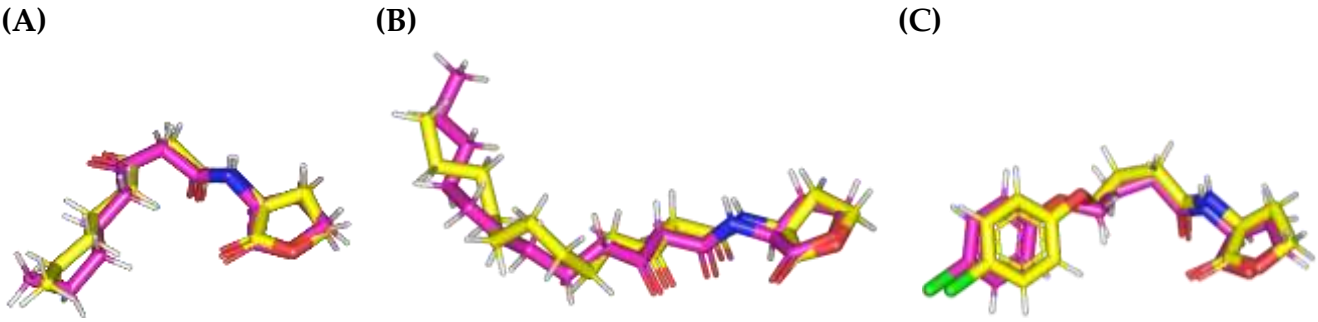


**Figure S6.** Superimposing the co-crystallized (magenta sticks) and redocked (yellow sticks) ligands. (**A**) TraR *A. tumefaciens*; (**B**) QscR *P. aeruginosa*; (**C**) CviR *C. violaceum* for validating the adopted directed docking protocol.